Topology optimization method applied to the design of electromagnetic devices: focus on convexity issues

Th. Labbé*, F. Glineur**, B. Dehez***

* F.R.S.-FNRS fellow, Université Catholique de Louvain/Centre for Research in Mechatronics, Louvain-la-Neuve, BELGIUM

** Université Catholique de Louvain/Center for Operations Research and Econometrics, Louvain-la-Neuve, BELGIUM

*** Université Catholique de Louvain/Centre for Research in Mechatronics, Louvain-la-Neuve, BELGIUM

***Abstract*—To perform parameter and shape optimization, an initial topology is required which affects the final solution. Topology optimization methods have the advantage to release this constraint. They are based on a splitting of the design space into cells, in which they attempt to distribute optimally some given materials.**

In this paper, the optimization is based on a discrete formulation of the Maxwell equations obtained thanks to a finite element model. The gradient of the objective function is computed immediately from this discrete form, which is more convenient than the adjoint variable method. A line-search method (steepest descent direction) is then applied. The step size is computed by a simple and quick algorithm, to achieve good and fast convergence.

Several convexity issues were already highlighted in topology optimization. We explain how we can face some of them by performing the optimization on a variable linked to the permeability by a given mapping. This mapping actually affects the value of intermediate materials and must be selected carefully to avoid the algorithm to be trapped in some local minimizers.

In order to illustrate the concepts presented along the paper, the method is applied for the topology optimization of a linear reluctant actuator.

I. INTRODUCTION

Optimization methods differentiate themselves from the design parameters on which they are performed. Parameter optimization is concerned with some dimensions of the drive topology, such as the length of a tooth. However, the range of solutions that may be obtained is limited by the topology fixed initially. Shape optimization experiences the same issue at a lower level.

In topology optimization, the design space is split into cells. The method is then concerned with distributing predefined materials into the cells, such as air, copper or iron. The design parameters are thus the electric and magnetic properties in each cell. The main advantage of this approach is that no initial topology is required and that the design parameters enable any topology to be represented. However, the resolution is limited to the number of cells, which must be kept quite low to limit the number of design parameters.

In this paper, the problem is first formulated, which includes the development of the finite element model for the field computation and the description of the constraints linked to the predefined materials. Next, the gradient based optimization method is described. We explain how the gradient can be computed directly from the discrete equations of the finite element model. This method gives the same results as the adjoint variable method used in [1]-[4] but is more convenient.

Then, some convexity issues are discussed. The optimization is usually performed on a design variable linked to the permeability by a given mapping, rather than on the permeability itself. This mapping actually affects the convexity of the problem. Different mapping were introduced in [4]-[10] but never because of convexity problems. Thereby, we suggest a mapping specifically selected to deal with some of the convexity issues.

Finally, the concepts developed along the paper are illustrated through an application of the method for the optimization of a reluctant linear actuator.

II. PROBLEM FORMULATION

This section is dedicated to the formulation of the topology optimization problem in the particular case of a magnetostatic problem. To evaluate the objective function, the magnetic fields are computed thanks to a finite element model. The method described in this paper does not rely on an independent finite element solver, but it focuses directly on the finite element equations. The space splitting into cells is used directly as the finite element mesh.

This section includes the development of the finite element equations and the description of the optimization constraints linked to the materials.

A. Finite element model

The finite element model is based on the following Maxwell equations:

$$\nabla \times H = J, \tag{1}$$

$$B = \nabla \times A, \tag{2}$$

$$B = \mu H, \tag{3}$$

with H and B the magnetic field, J the current density, A the vector potential and μ the permeability.

These equations can be grouped into one:

$$\nabla \times \left(\frac{1}{\mu} \nabla \times A \right) = J. \tag{4}$$

The weak formulation is obtained by multiplying each side of (4) by an arbitrary vector potential $\hat{A}$ and by integrating them over the whole domain:

$$\int_\Omega \hat{A}\nabla\times\left(\frac{1}{\mu}\nabla\times A\right)d\Omega = \int_\Omega \hat{A}Jd\Omega. \quad (5)$$

This weak formulation remains equivalent to (4) since it must be verified for any $\hat{A}$. The integration by parts gives:

$$\int_\Omega \nabla\times\left(\hat{A}\left(\frac{1}{\mu}\nabla\times A\right)\right)d\Omega + \int_\Omega\left(\nabla\times\hat{A}\right)\cdot\left(\frac{1}{\mu}\nabla\times A\right)d\Omega = \int_\Omega \hat{A}Jd\Omega. \quad (6)$$

The first term can be developed thanks to the Kelvin-Stokes theorem:

$$\int_\Omega \nabla\times\left(\hat{A}\left(\frac{1}{\mu}\nabla\times A\right)\right)d\Omega = \oint_{\partial\Omega}\hat{A}\left(\frac{1}{\mu}\nabla\times A\right)dS. \quad (7)$$

This integral actually equals to zero. Indeed, we consider situations were either the normal or the parallel component of B is zero on the boundary. In the first case, we can assume homogeneous conditions on the vector potential A which also apply to $\hat{A}$. In the second case, the curl of A is zero.

The weak formulation reduces then to:

$$\int_\Omega\left(\nabla\times\hat{A}\right)\cdot\left(\frac{1}{\mu}\nabla\times A\right)d\Omega = \int_\Omega \hat{A}Jd\Omega. \quad (8)$$

To derive the discrete formulation, we approximate the vector potentials A and $\hat{A}$ by discrete values at each node of the mesh:

$$A = \sum_{i=1}^{n} u_i\tau_i, \quad (9)$$

$$\hat{A} = \sum_{i=1}^{n} \hat{u}_i\tau_i, \quad (10)$$

with n the number of nodes and u_i the vector potential on the node i. τ_i is a shape function equal to 1 on node i and zero on the other nodes. Pyramidal functions are used since the mesh is triangular.

The reluctivity $\nu = \frac{1}{\mu}$ and the current density J are approximated by a discrete value in each cell:

$$\nu = \sum_{i=1}^{m} \nu_i\phi_i, \quad (11)$$

$$J = \sum_{i=1}^{m} j_i\phi_i, \quad (12)$$

with m the number of cells and ϕ_i a shape function equal to 1 on the cell i and 0 everywhere else. These approximations are inserted in (8) to obtain:

$$\sum_{i=1}^{n}\sum_{j=1}^{n}\sum_{k=1}^{m}\hat{u}_i u_j\nu_k\int_\Omega(\nabla\times\tau_i)\cdot(\phi_k\nabla\times\tau_j)d\Omega = \sum_{i=1}^{n}\sum_{k=1}^{m}\hat{u}_i j_k\int_\Omega\tau_i\phi_k d\Omega. \quad (13)$$

This equation must be satisfied for any vector potential $\hat{A}$, and thus for any value of $\hat{u}_i$. We can thus write:

$$\sum_{j=1}^{n}\sum_{k=1}^{m}u_j\nu_k\int_\Omega(\nabla\times\tau_i)\cdot(\phi_k\nabla\times\tau_j)d\Omega = \sum_{k=1}^{m}j_k\int_\Omega\tau_i\phi_k d\Omega \qquad \forall i. \quad (14)$$

Since the shape functions are known, the integral terms can be computed to obtain the following matrices:

$$M_{ij}(\nu) = \sum_{k=1}^{m}\nu_k\int_\Omega(\nabla\times\tau_i)\cdot(\phi_k\nabla\times\tau_j)d\Omega, \quad (15)$$

$$C_{ik} = \int_\Omega\tau_i\phi_k d\Omega. \quad (16)$$

The vector potential is then computed from the current density j and the reluctivity ν by the following linear system:

$$\sum_{j=1}^{n}M_{ij}(\nu)u_j = \sum_{k=1}^{m}C_{ik}j_k \quad\Leftrightarrow\quad M(\nu)u = Cj. \quad (17)$$

The M matrix can be actually rewritten to make ν appears. The development is made for the two dimensions x and y, but it can be easily generalized for three dimensions. Assuming that the current J is on the z-axis, it comes from (15):

$$M_{ij}(\nu) = \sum_{k=1}^{m}\nu_k\int_\Omega\phi_k\left(\frac{\partial\tau_i}{\partial y}\frac{\partial\tau_j}{\partial y}+\frac{\partial\tau_i}{\partial x}\frac{\partial\tau_j}{\partial x}\right)d\Omega. \quad (18)$$

The ϕ_k shape functions are equal to 1 on cell k and zero everywhere else. The integral can thus be rewritten as:

$$M_{ij}(\nu) = \sum_{k=1}^{m}\nu_k\left(\int_{\Delta_k}\frac{\partial\tau_i}{\partial y}\frac{\partial\tau_j}{\partial y}+\int_{\Delta_k}\frac{\partial\tau_i}{\partial x}\frac{\partial\tau_j}{\partial x}\right)d\Omega, \quad (19)$$

with Δ_k the domain of cell k. We can now write:

$$\int_{\Delta_k}\frac{\partial\tau_i}{\partial y}\frac{\partial\tau_j}{\partial y}d\Omega = \frac{\partial\tau_i}{\partial y}^{(k)}\frac{\partial\tau_j}{\partial y}^{(k)}S_{\Delta_k}, \quad (20)$$

with S_{Δ_k} the surface of cell k and $\frac{\partial\tau_i}{\partial y}^{(k)}$ the derivative of τ_i on it. Indeed, the derivatives of the shape functions are constant on a cell since we use pyramidal functions. The matrix M can then be computed by:

$$M_{ij}(\nu) = \sum_{k=1}^{m}A_{ik}\nu_k A_{kj}^T + \sum_{k=1}^{m}B_{ik}\nu_k B_{kj}^T, \quad (21)$$

$$M(\nu) = AV\,A^T + BV\,B^T, \quad (22)$$

with V the matrix containing ν on its diagonal and A and B given by:

$$A_{ik} = \sqrt{S_{\Delta_k}} \frac{\partial \tau_i}{\partial y}^{(k)}, \quad (23)$$

$$B_{ik} = \sqrt{S_{\Delta_k}} \frac{\partial \tau_i}{\partial x}^{(k)}. \quad (24)$$

The system of discrete equations for the optimization problem is thus:

$$(AV\,A^T + BV\,B^T)u = C\,j. \quad (25)$$

The Maxwell equations are actually hidden in this expression:

$$b_x = A^T u, b_y = -B^T u \leftrightarrow B = \nabla \times A, \quad (26)$$

$$h_x = \nu b_x, h_y = \nu b_y \leftrightarrow H = \nu B, \quad (27)$$

$$Ah_x + Bh_y = -C\,j \leftrightarrow \nabla \times H = J. \quad (28)$$

Thanks to (25), the objective function can be computed from the reluctivity ν and the current density j. Indeed, if they are needed, the vector potential A is calculated by $u = M^{-1}(\nu)\,j$ and the magnetic fields H and B may be obtained from u thanks to (26) to (28). A cost on the materials must be reflected on ν and j.

B. Material constraints

The optimization can often be performed using only the three materials described in Table 1. Indeed, it is often possible to take advantage of symmetries to avoid the necessity to use an addition material having a negative current density. In addition, the design space is reduced.

TABLE I. TABLE 1: ELECTRIC AND MAGNETIC PROPERTIES OF THE MATERIALS

Material	Permeability (μ)	Current Density (j)
Air	μ_0	0
Iron	$\mu_0\mu_r$	0
Copper	μ_0	J

As explained in section 4, it is interesting for convexity issues to perform the optimization on a parameter p linked to the permeability by a specific mapping $\mu = g(p)$, rather than on the permeability itself, with the following characteristics: $g(p=0) = \mu_0$ and $g(p=1) = \mu_0\mu_r$. The optimization problem is thus:

$$minf(p, j) \quad (29)$$

$$j_i \geq 0 \quad (30)$$

$$p_i \geq 0 \quad (31)$$

$$p_{i,max}\,j_i + j_{i,max}\,p_i \leq j_{i,max}\,p_{i,max} \quad (32)$$

$$j_i \leq j_{i,max} \quad (33)$$

$$p_i \leq p_{i,max} \quad (34)$$

with f the objective function.

Some materials may be forbidden in some cells. For instance, the rotor of a reluctant motor cannot contain current. That is the reason why we write $j_{i,max}$ the maximum current density that cell i can contain (J if the element can contain copper, 0 otherwise). In the same way, we note $p_{i,max} = 1$ for a cell that may contain iron, $p_{i,max} = 0$ otherwise. The feasible domain for the electromagnetic properties p and j in a cell is represented on Fig.1.

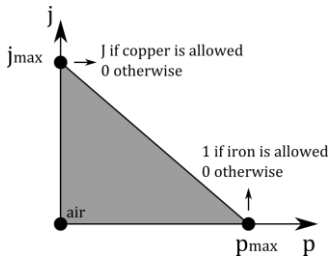

Fig. 1. Feasible domain for the magnetic properties p and j in a cell

III. OPTIMIZATION ALGORITHM

The optimization algorithm is based on a line-search method which uses the steepest descent direction (the opposite direction to the gradient). At each iteration, the design variables are updated in this way:

$$j^{(i)} = j^{(i-1)} + \alpha d_j, \quad (35)$$

$$p^{(i)} = p^{(i-1)} + \alpha d_p, \quad (36)$$

with $d_j = -\frac{\partial f}{\partial j}$ and $d_p = -\frac{\partial f}{\partial p}$ the j and p components of the descent direction and α the step size.

The algorithm requires thus an evaluation of the gradient of the objective function at each iteration. This section starts with the sensitivity analysis. Next, a method to manage the constraints related to the feasible domain in each cell is explained. Finally, we describe an algorithm to compute a reasonable step size in the steepest descent direction.

A. Sensitivity analysis

The gradient related to the design variables is a really good tool in optimization. In topology optimization, the adjoint variable method is widely used to compute the gradient [1]-[4]. Other authors compute the gradient from the mutual energy [11]. In this paper, the gradient is calculated immediately from the objective function in its matrix product form. The result is exactly equivalent but this method is more convenient and intuitive.

The objective function of a magnetostatic optimization problem depends at least partly on the vector potential, which is computed by inverting the $M(\nu)$ matrix. Thereby, it is interesting to study the gradient of $M^{-1}(\nu)$. We differentiate the following expression:

$$M(\nu)\,M(\nu)^{-1} = I, \quad (37)$$

which gives:

$$M(\nu)\frac{\partial M_{ij}(\nu)^{-1}}{\partial \nu_k} = -\frac{\partial M_{ij}(\nu)}{\partial \nu_k} M(\nu)^{-1}, \quad (38)$$

$$\frac{\partial M_{ij}(\nu)^{-1}}{\partial \nu_k} = -M(\nu)^{-1}\frac{\partial M_{ij}(\nu)}{\partial \nu_k} M(\nu)^{-1}. \quad (39)$$

From (21), we can write:

$$\frac{\partial M_{ij}(\nu)}{\partial \nu_k} = A_{ik}A_{kj}^T + B_{ik}B_{kj}^T. \quad (40)$$

This result enables to compute easily the gradient of the objective function with respect to the design variables.

B. Constrained optimization

Fig.2 illustrates an iteration of the line-search method for two cells. The feasible domains are plotted and the initial points within those domains are represented by grey circles. The steepest descent direction is pointed out by black arrows.

There are two different cases where the constraints get involved:

• If a point lies initially on a constraint and if its descent direction points out of the feasible domain (a), then the direction must be projected on the constraint.

• If a point lies initially inside the feasible domain and the step size is large enough to put it out of the domain, then there are two possibilities, represented for cell (b):

(a) The new point is placed where the constraint was met.

(b) The new point is the projection of the outside point on the constraint. This is equivalent to project the gradient when the constraint is met and then to continue with the projected gradient. This is the method we use in this paper.

C. Step size computation

Choosing a right step size is important. Indeed, if steps are too short then the algorithm will be very slow. On the other hand, too large steps can lead to instability and could worsen the objective function value. Obviously, the optimal step size is the one that minimizes the objective function in the steepest descent direction.

Finding the optimal step is really time consuming. We will rather be satisfied with a reasonable good step, which can be computed by the following method:

• Try with an initial guess of the step size. This initial guess is computed based on the previous step :

(a) Count in how many cells one of the three corners of the feasible domain was reached at the previous step.

(b) Compute a step size for which a corner is reached in the same number of cells.

• Compute the objective function and compare it with its value at the initial point. There are two possibilities :

(a) The value obtained is better than at the initial point, a larger step may be better : multiply the step by a factor θ as long as it decreases the objective function.

(b) The value obtained is worse than at the initial point, the step size is thus too large : divide the step by the factor θ as long as it decreases the objective function.

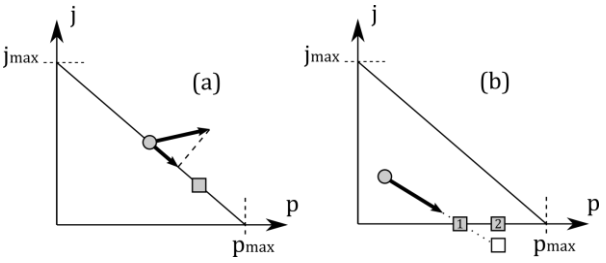

Fig. 2. Algorithm iteration for two cells

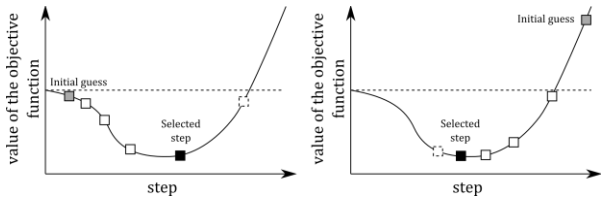

Fig. 3. Selection of the step based on an initial guess

The method is illustrated on Fig.3 for the two cases. It is really quick and works very well. It enables to avoid too short as well as too large steps and ensures a reduction of the objective function at each step, which guarantees a stable convergence.

In [2] and [12], an "ON/OFF" method is suggested: the materials are changed in all the cells according to the inverse of the gradient. This is similar to the selection of a very large step size for which the solution goes in a corner of the feasible domain in all the cells. Since this can lead to instability, they need to use some heuristic smoothers after each step.

IV. CONVEXITY ISSUES

An important issue in optimization is to prove that a problem minimizer is global. This is often impossible, excepted when the problem is convex: in that case, every local minimum is a global minimizer, and the set of all those minimizers is convex.

For topology optimization, lack of convexity has already been experimentally observed. For instance, the solution of a rotor optimization in [6] depends on the initial solution used to start the line-search algorithm.

As explained before, the optimization is performed on a variable p linked to the permeability by a given mapping, rather than on the permeability itself. The convexity of the optimization problem is affected by the objective function, but also by the mapping selected.

In the literature, different mapping are suggested. In [5], a geometrical relation of this form is used:

$$\mu = \mu_0(\mu_r)^p, \quad (41)$$

where p is the design variable used to control the permeability in the cell. When p varies from 0 to 1, μ varies from μ_0 to μ_r. In [4], [6], [7], a quadratic mapping is recommended:

$$\mu = \mu_0(1+(\mu_r-1)p^n), \quad (42)$$

with n a penalty factor comprised between 2 and 4. Finally, some authors put a lot of effort in finding a

mapping physically explainable and based on the equivalent permeability of a microstructure [8]-[10]. This is called the *homogenization theory* and was first developed for topology optimization of mechanical structure [13].

However, in the literature, the aim of the mapping is usually described vaguely as a way to enhance the speed and performances of the algorithm. The convexity issue is never highlighted to justify a mapping selection.

In this paper, we suggest the following mapping:

$$\mu = \mu_0 \frac{1+(\mu_r-1)(1-a)p}{1+(\frac{1}{\mu_r}-1)ap}, \qquad (43)$$

where $a \in [-\infty, \frac{\mu_r}{\mu_r - 1}[$ is a parameter. This mapping was selected because the convexity can be directly improved for cells moving between copper and iron by decreasing a.

This feature can be explained by examining the possible values that the permeability μ and the current density j can take. Indeed, since the feasible domain for p and j remains a triangle, the surface of the possible values for μ and j changes according to a, which is illustrated on Fig.4.

When a cell is moving between copper and iron, its design parameter p and j lie on the slanted constraint of its feasible domain. The electromagnetic properties μ and j in the cell follow then the curves represented on Fig.4 for different values of a. When a decreases, cells containing intermediate materials becomes more valuable since their electromagnetic properties are higher. The objective function gets thus a more convex shape.

To approach the global minimizer, the algorithm must thus be started with a low value of a. Thereby, we avoid the solution to be trapped in a corner of the feasible domain. However, the solution obtained will contain some intermediate materials, but they can be removed by increasing progressively the value of a.

The mapping proposed in this paper is thus a useful tool to face with convexity problems for cells moving between copper and iron. However, it has no effect on convexity issues that may appear when moving between air and copper or between air and iron.

V. Application

In this section, the method is applied for the optimization of a linear actuator. Fig.5 shows a schematic view of the actuator in its two extreme positions and a zoom of the design space. The aim is to maximize the force on the rotor and thus the difference of magnetic coenergy between those two positions.

The objective function is thus $minf = \frac{1}{2}\int_\Omega J(A_1 - A_2)$, where A_1 and A_2 are the vector potentials for the opposition and the conjunction positions while J is the current density.

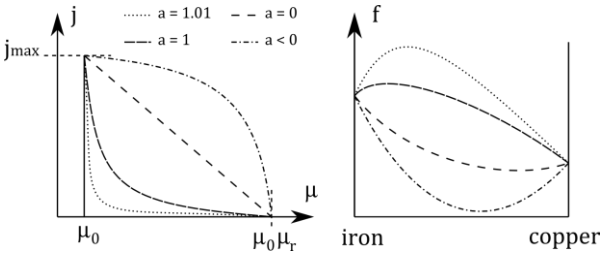

Fig. 4. Domain of the possible values for μ and j and illustration of the convexity evolution in function of a

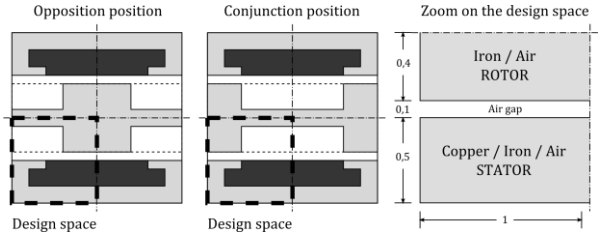

Fig. 5. Linear drive

In a discrete form, it becomes:

$$f = \frac{1}{2} j^T C^T (u_1 - u_2) = \frac{1}{2} j^T C^T (M^{-1}(\nu_1) - M^{-1}(\nu_2))Cj. \qquad (44)$$

The derivatives of the objective function are:

$$\frac{\partial f}{\partial j} = C^T (M^{-1}(\nu_1) - M^{-1}(\nu_2))Cj = C^T (u_1 - u_2), \qquad (45)$$

$$\frac{\partial f}{\partial p_k} = \frac{\partial f}{\partial \nu_k}\frac{\partial \nu_k}{\partial p_k} = \frac{1}{2}\left((u_1-u_2)^T \frac{\partial M(\nu)}{\partial \nu_k}(u_1-u_2)\right) \left(\frac{(\frac{1}{\mu_r}-1)a-(\mu_r-1)(1-a)}{\mu_0(1+(\mu_r-1)(1-a)p)^2}\right). \qquad (46)$$

Fig.6 regroups the optimization results for different initial solutions, mesh sizes and value of a. Here are some comments based on these results.

- The optimization was performed with the parameter $a = 0$. Indeed, this value was low enough to obtain a convex behaviour: the stator part optimized with different initial solutions and mesh sizes are identical ((a), (b) and (c)).
- Different shapes are obtained for the rotor due to the lack of convexity. The concavity shape of the objective function is highlighted on Fig.7 where its evolution is plotted when moving from (a) to (b). The mapping and the value of a has no influence on this concave behaviour.
- The solution (d) was obtained by starting with the solution (c) and continuing the optimization while increasing a. Thereby, the value of intermediate materials decreases and they disappear in the solution eventually obtained.

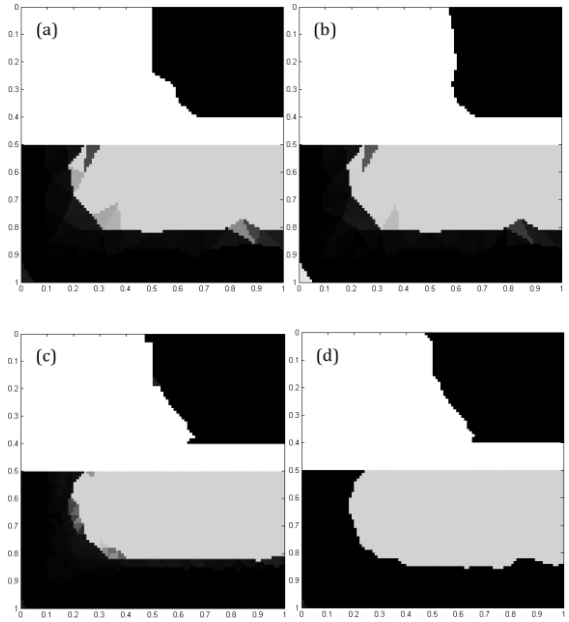

Fig. 6. Optimization results :
(a) coarse mesh, $a = 0$
(b) same mesh as (a), other initial solution, $a = 0$
(c) fine mesh, same initial solution as (a), $a = 0$
(d) initial solution (c) intermediate material removal by increasing a

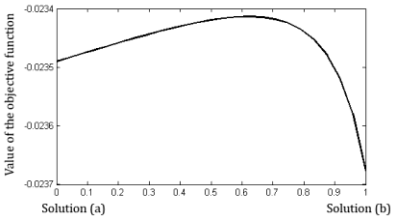

Fig. 7. Concavity illustration for the rotor

VI. CONCLUSION

In conclusion, several aspects of topology optimization were examined along this paper.

First, the optimization problem was defined: the Maxwell equations were transformed into a discrete form and the constraints linked to the materials were described.

Next, the optimization algorithm was explained. The algorithm is based on a line-search method which uses the steepest descent direction. We proposed a new method to compute the gradient directly from the discrete form of the objective function, which gives the same results but is more intuitive and convenient than the adjoint variable method. The material-related constraints were handled and an algorithm was detailed for the step size computation.

Then, the convexity issues linked to the topology optimization were discussed. For cells moving between iron and copper, it was shown that the convexity can be affected through the mapping between the permeability and the design parameter used to represent it. Several mappings have already been suggested in the literature but the reasons for their utilization were never convexity issues. That is the reason why we introduced a new mapping focusing specifically on convexity. This mapping contains a parameter that can be used to enhance the convexity of the objective function since it modifies the value of intermediate materials.

Finally, all those aspects were illustrated by the optimization of a linear reluctant actuator.

REFERENCES

[1] D. Dyck and D. Lowther, "Design of electromagnetic devices usingsensitivities computed with the adjoint variable method," in Second International Conference on Computation in Electromagnetics, Apr. 1994, pp. 231–234.

[2] Y. Okamoto, K. Akiyama, and N. Takahashi, "3-d topology optimization of single-pole-type head by using design sensitivity analysis," IEEE Transactions on Magnetics, vol. 42, no. 4, pp. 1087–1090, Apr. 2006.

[3] J. Yoo, S. Yang, and J. Choi, "Optimal design of an electromagnetic coupler to maximize force to a specific direction," IEEE Transactions on Magnetics, vol. 44, no. 7, pp. 1737–1742, Jul. 2008.

[4] S. Wang, S. Park, and J. Kang, "Multi-domain topology optimization of electromagnetic systems," COMPEL : The International Journal for Computation and Mathematics in Electrical and Electronic Engineering, vol. 23, no. 4, pp. 1036–1044, 2004.

[5] D. Dyck and D. Lowther, "Automated design of magnetic devices by optimization material distribution," IEEE Transactions on Magnetics, vol. 32, no. 4, pp. 1188–1193, May 1996.

[6] J. Byun, I. Park, and S. Hahn, "Topology optimization of electrostatic actuator using design sensitivity," IEEE Transactions on Magnetics, vol. 38, no. 2, pp. 1053–1056, Mar. 2002.

[7] J. Byun, J. Lee, I. Park, and H. Lee, "Inverse problem application of topology optimization method with mutual energy concept and design sensitivity," IEEE Transactions on Magnetics, vol. 36, no. 4, pp. 1144–1147, Jul. 2000.

[8] D. Dyck and D. Lowther, "Composite microstructure of permeable material for the optimized material distribution method of automated design," IEEE Transactions on Magnetics, vol. 33, no. 2, pp. 1828–1831, Mar. 1997.

[9] J. Yoo, "Modified method of topology optimization in magnetic fields," IEEE Transactions on Magnetics, vol. 40, no. 4, pp. 1796–1800, Jul. 2004.

[10] J. Yoo, N. Kikuchi, and J. Volakis, "Structural optimization in magnetic devices by the homogenization design method," IEEE Transactions on Magnetics, vol. 36, no. 3, pp. 574–580, May 2000.

[11] J. Byun and S. Hahn, "Topology optimization of electrical devices using mutual energy and sensitivity," IEEE Transactions on Magnetics, vol. 35, no. 5, pp. 3718–3720, Sep. 1999.

[12] N. Takahashi, K. Akyama, D. Miyagi, and Y. Kanai, "Advanced optimization of standard head model with higher writing field and higher field gradient using 3-d on/off method," IEEE Transactions on Magnetics, vol. 44, no. 6, pp. 966–969, Jun. 2008.

[13] M. Bendsøe and N. Kikuchi, "Generating optimal topologies in structural design using a homogenization method," Computer Methods in Applied Mechanics and Engineering, vol. 71, pp. 197–224, 1988.